Science Advances
AAAS

Supplementary Materials for

Distinct septo-hippocampal cholinergic projections separately mediate stress-induced emotional and cognitive deficits

Jian-Lin Wu *et al.*

Corresponding author: Tian-Ming Gao, tgao@smu.edu.cn

Sci. Adv. **10**, eado1508 (2024)
DOI: 10.1126/sciadv.ado1508

This PDF file includes:

Supplementary Materials and methods
Figs. S1 to S15

Supplemental material

Materials and Methods

Mice

We used (all males, aged 8–12 weeks) ChAT-ires-cre mice (Jax No. 006410, a gift from Li Xiaoming at Zhejiang University). Male C57BL/6 J mice (aged 8–10 weeks) were obtained from the Southern Medical University Animal Center (Guangzhou, China). All mice were maintained on a 12-h:12-h light:dark cycle in a temperature controlled room (21-25 ℃). Food and water were available ad libitum. Behavioral testing was performed during the light cycle between 10:00 A.M. and 5:00 P.M. All animal procedures were performed in accordance with the institutional guidelines of Southern Medical University, Guangzhou, and the governmental regulations of China. Efforts were made to minimize animal suffering and to reduce the number of animals used.

Virus preparation

For fiber photometry recording of Ca^{2+} signaling, we used AAV-Ef1α-Dio-GCaMP6m (titer, 5.99×10^{12} v.g./mL) and AAV-Ef1α-Dio-axon-GCaMP6s (titer, 2.86×10^{12} v.g./mL), which were purchased from BrainVTA, Wuhan, China. For optogenetic modulation of neurons and their projection, we used AAV-Ef1α-Dio-ChR2-mCherry (titer, 1.09×10^{12} v.g./mL), AAV-Ef1α-Dio-mCherry (titer, 1.42E $\times 10^{12}$ v.g./mL), AAV-Ef1α-Dio-eNpHR-EGFP (titer, 5.54×10^{12} v.g./mL), and AAV-Ef1α-Dio-EGFP (titer, 3.81×10^{12} v.g./mL), which were purchased from Sunbio Medical Biotechnology, Shanghai, China. For chemogenetic modulation of neurons and their projection, we used AAV-Ef1α-Dio-hM4Di-mCherry (titer, 6.61×10^{13} v.g./mL) and AAV-Ef1α-Dio-hM3Dq-mCherry (titer, 2.45×10^{13} v.g./mL), which were purchased from BrainVTA, Wuhan, China. For antrograde tracing, we used AAV-nEf1α-FDio-eYFP (titer, 5.00×10^{12} v.g./mL) and AAV_{retro}-Ef1α-

Dio-FLP (titer, 2.46 × 10^{12} v.g./mL). For retrograde tracing, we used AAV_{retro}-Ef1α-Dio-mCherry (titer, 5.84 × 10^{12} v.g./mL) and AAV_{retro}-Ef1α-Dio-eYFP (titer, 6.08× 10^{12} v.g./mL), which were purchased from BrainVTA, Wuhan, China. To examine the input domains of these two distinct subpopulations of cholinergic neurons, we used RV-Envs-ΔG-mCherry (titer, 5.84 × 10^{12} v.g./mL), AAV_{retro}-Ef1α-Dio-FLP, rAAV-nEf1α-FDio-oRVG(19G), and rAAV-nEf1α-FDio-EGFP-T2A-TVA, which were purchased from BrainVTA, Wuhan, China. For recording of ACh release in hippocampus, we used AAV-hSyn-gACh3.8 (titer, 2.83 × 10^{12} v.g./mL), which were purchased from BrainCase, Shenzhen, China.

Stereotaxic surgery

Stereotaxic brain injection was performed using a stereotactic instrument (RWD, China) under anesthesia induced by an intraperitoneal injection of pentobarbital (75 mg/kg). A volume of 100–300 nl of virus (depending on the expression strength and viral titre) was injected through calibrated glass microelectrodes connected to an infusion pump (Nanoliter 2010 Injector, WPI) at a rate of 50 nl/min. The pipette was left in the injection site for approximately 10 minutes following infusion to prevent virus overflow.

For the MS/vDB injection, 200-300 nl AAV virus was slowly injected into the MS/vDB of ChAT-ires-Cre mice (+1.6 mm AP; ±0.65 mm ML; -4.0 mm DV; AP, ML and DV denote anteroposterior, mediolateral and dorsoventral distance from bregma, respectively) with an angle of 10 °outward in the coronal plane.

For retrograde tracing, we bilaterally injected 200 nL of the following viruses: AAV_{retro} -Ef1α-Dio-mCherry into vHPC (-3.0 mm AP; ±3.6 mm ML; -3.7 mm DV) and AAV_{retro}-Ef1α-Dio-eYFP into dHPC (-1.4 mm AP; ±1.5 mm ML; -1.3 mm DV) of ChAT-ires-Cre mice. To trace the projection of

different MS cholinergic neurons, 200 nL of AAV_{retro}-Ef1α-Dio-Flp was injected into the vHPC or dHPC, and 200 nL of AAV-nEf1α-FDio-eYFP was injected into the MS/vDB of the same mouse. For optogenetic activation or inhibition of cholinergic neurons in the MS/vDB, an optical fiber (200 μm O.D., NA = 0.37; Newdoon) was implanted along the same track over the MS/vDB at a depth of -3.8 mm. For optogenetic activation of cholinergic fibers in the dHPC or vHPC, an optical fiber was implanted unilaterally into the dHPC (-1.4 mm AP; ±1.5 mm ML; -1.1 mm DV) or vHPC (-3.0 mm AP; ±3.6 mm ML; -3.5 mm DV). For optogenetic or chemogenetic inhibition of cholinergic fibers in the dHPC or vHPC, optical fibers or guide cannulas were bilaterally implanted into the dHPC or vHPC.

Fiber photometry recording

For calcium signal recording in the MS/vDB, AAV-Dio-GCaMP6m virus was injected into the MS/vDB of ChAT-ires-Cre mice, and an optical fiber was inserted toward the MS/vDB through craniotomy. For calcium signal recording of cholinergic fibers in the dHPC or vHPC, AAV-Dio-axon-GCaMP6s virus was injected into the MS/vDB of ChAT-ires-Cre mice, and 4 weeks later, an optical fiber was implanted unilaterally into the dHPC or vHPC. Mice were housed for at least 2 weeks to recover. Fiber photometry experiments were performed as previously described. Briefly, a laser beam from a 488 nm laser (OBIS 488LS; Coherent) was reflected by a dichroic mirror (MD498; Thorlabs), focused by a 10 X objective lens (NA = 0.3; Olympus) and coupled to an optical commutator (Doric Lenses). An optical fiber (200 μm O.D., NA = 0.37, 3 m long) guided the light between the commutator and the implanted optical fiber. The laser power was adjusted at the tip of the optical fiber to the low level of ~30 μW to minimize bleaching. The excited fluorescence signals were bandpass filtered (MF525-39, Thorlabs) and converted to electrical signals by a

photomultiplier tube (R3896, Hamamatsu). An amplifier (C7319, Hamamatsu) was used to convert the current output of the photomultiplier tube to voltage signals, which were further filtered through a low-pass filter (40 Hz cutoff; Brownlee 440). The analog voltage signals were digitalized at 100 Hz using a Power 1401 digitizer and Spike2 software (CED, Cambridge, UK).

Photometry data were exported to MATLAB mat files for further analysis. Data were segmented based on behavioral events within individual trials. The fluorescence change (△ F/F) was calculated by (F-F0)/F0, where F0 is the baseline fluorescence signal averaged over the control time.

The stress procedures are detailed as follows:

(1) Foot-shock test. Animals were introduced into an acrylic box (30 x 32 x 35, L x W x H in cm) with a metal grid floor. In a single experimental session, four footshocks (0.7 mA; 1 s) were randomly delivered with intertrial intervals of 70-90 s;

(2) TRT. The tail of tested mice was chased and grabbed by hand. After grabbing, the mice were suspended in air for 10 s before being released into the cage.

(3) Social attack. We introduced a test male mouse into the home cage of an aggressive CD-1 mouse. Attack onset was defined as the time when an aggressive mouse attacked the test mouse for a period lasting at least 3 s.

(4) Intraoral infusion of quinine or sucrose. We implanted an intraoral cheek fistula following a previously described procedure. To examine the effect of quinine or sucrose delivery, 10 infusions of quinine solution (speed 20 μl/s and duration 0.5 s) were given within one recording session with random intervals ranging from 40 to 60 s.

(5) Elevate plus maze. Mice were placed in a standard EPM-sized maze, which consisted of two open arms (30 x 5 cm) and two enclosed arms (30 x 5 x 30 cm) extending from a central platform

(5 x 5 cm) at 90 degrees in the form of a plus. Mice were allowed to explore for 20 minutes, and every initiation time of closed-open arms across was determined by video scoring.

The reward procedures are detailed as follows:

(1) Sucrose lick. A mouse was water deprived for 12 h before it was placed in a chamber (20 x 20 x 22, L x W x H in cm) equipped with a contact lickometer connected to a bottle filled with 5% sucrose solution (w/v). The onset of mouse sucrose consumption was determined by lick signal recording from the lickometer.

(2) Food consumption. Mice were food deprived for 12 h before they were placed into the behavior chamber and habituated for 5 min. Then, a small pellet of food (~4 g per pellet) was placed. Videos were recorded 15-20 min per session from a camera placed overhead. Every initiation time for food intake was determined by video scoring.

Behavioral assays

Elevate plus maze. Mice were placed in a standard EPM-sized maze with a 650 lux light centered over the maze to promote avoidance. Mice were placed in the center region of the maze and were allowed to explore for 5 minutes while their behavior was recorded with an autonomous camera. For optogenetic studies, mice were allowed to explore for a 9-minute session in which there were three alternating 3-minute epochs (OFF-ON-OFF epochs), and light was delivered at the second 3 minutes. Behavior was analyzed with Ethovision XT video tracking software (Noldus Information Technologies).

Open field test. Mice were placed in a box (40 x 40 x 30, L x W x H in cm) with bright light (650 lux) centered over the center zone. Mice were allowed to explore for 5 minutes. For optogenetic studies, mice were allowed to explore for a 9-minute session in which there were three alternating

3-minute epochs (OFF-ON-OFF epochs), and light was delivered at the second 3 minutes. Behavior was recorded and analyzed by Ethovision XT video tracking software (Noldus Information Technologies).

Real-time place avoidance test (RTPA). The RTPA contained a transparent plastic chamber (50 x 53 x 20, L x W x H in cm) and was divided into two equal compartments. One of these was assigned as the photostimulated zone (counterbalanced between animals). At the start of the 20 min session, mice were placed in the nonstimulated side of the chamber. Light was delivered every time the mouse crossed to the side of the photostimulated chamber. Behavior was recorded and analyzed by Ethovision XT video tracking software (Noldus Information Technologies).

Conditioned place preference (CPP). Individual mice were placed in a CPP apparatus comprising three side chambers (57.15 x 22.5 x 30.5, L x W x H in cm). One side chamber had a black bar on the walls and metal grill floor, and the other side chamber had a black spot on the walls and a plastic floor. Mouse locomotion was tracked using a video system and analyzed offline. The entire CPP test consisted of 3 phases: preconditioning phase on Day 1, conditioning phase on Day 2 and Day 3, and test phase on Day 4. During the preconditioning phase, individual mice were allowed to freely explore the entire apparatus for 15 min. Any mouse that exhibited a preference for one of the side chambers (greater than 2 min difference) was excluded from further experiments. During the conditioning phase, mice were confined in one side chamber for 15 min with light delivered and then restrained in another chamber for 15 min without light delivery. During the test phase, the mice were allowed to freely explore the entire apparatus for 15 min. Behavior was recorded and analyzed by Ethovision XT video tracking software (Noldus Information Technologies). The place preference index (%) was calculated as follows: 100 x (Time spent in the light-paired chamber–Time spent in

the light-unpaired chamber)/(Time spent in either chamber).

Morris water maze test. The water maze consisted of a circular tank (Ø1 m) containing opaque water (~21 ℃). The maze was divided virtually into four quadrants, with one containing a hidden platform (Ø10 cm) present 1 cm below the water surface. Mice were trained to find the platform, orienting by three extramaze cues placed asymmetrically as spatial references. During acquisition, animals were placed into the water in a quasirandom fashion to prevent strategy learning. Mice were allowed to search for the platform for 90 s; if the mice failed to identify the platform within 90 s, they were guided gently onto the platform and allowed to stay there for 30 s before the initiation of the next trial. After the completion of four trials, the mice were dried and placed back into their home cages. Mice were trained for four trials per day for 5 consecutive days. Escape latency was measured as the time taken for the animal to locate the hidden platform in target quadrant Q1. For spatial probe trials, which were conducted 24 h after the last training session (Day 6), the platform was removed, and mice were allowed to swim for 90 s. The drop position was at the border between the third and fourth quadrant, with the mouse facing the wall at the start. Data are given as the percentage of time spent in quadrant Q1, the number of platform crossings, and the swimming speed. Swimming behavior was captured by a camera (model WVBP334, Panasonic), and the video signal was analyzed using EthoVision 7.0 (Noldus Information Technology).

Chronic Restraint Stress. Mice were subjected to CRS by placing them in a restraint cylinder fitted closely to body size and drilled with holes to allow free breathing for 1 session per day at approximately 2 PM for 2 hours per session for 10 consecutive days. The control mice were transferred in their home cages to the experimental room at 2 PM, gently handled for 5 minutes, and returned back to the holding room approximately 2 hours later for 10 consecutive days.

Light delivery

For light stimulation during behavioral assays, a 473 nm (blue light) or 593 nm laser (yellow light) was connected to a patch cord with a pair of FC/PC connectors at each end. This patch cord was connected through a fiber optic rotary joint (which allows free rotation of the fiber) with another patch cord with an FC/PC connector on one side and a ferrule connection on the other side (matching the size of the ferrule glued to the optic fiber implanted in the mouse). The optic fiber implanted in the mouse was connected to the optic patch cord. Blue light was delivered at 5 mW (in 20 Hz, 10 ms light pulses 10-second on–off cycle) to manipulate cell bodies and 15 mW for fiber manipulation. Yellow light was delivered at the same power as blue light but using a 9 s-on, 1 s-off process.

Drug delivery

For mAChR antagonist infusion, the solution consisted of DAU5884 (5 μM, Sigma–Aldrich, USA) dissolved in ACSF. For all hM4Di or hM3Dq mice, 5 μM clozapine-N-oxide (CNO, Sigma, USA) was used. Thirty minutes before the behavioral assays, 0.3 μl of solution was infused via infusion cannulas at a flow rate of 0.1 μl/min. The infusion cannulas (62203, RWD, China, length C = 0 mm, G = 3.0 mm for vHPC or 1.2 mm for dHPC) were connected via polyethylene tubing (62302, RWD, China) to 10-μl microsyringes (Hamilton, Reno, NV) mounted on a microinfusion pump (RWD200, China). To allow for the diffusion of the drug, the infusion cannulas were kept in place for 5 min before being replaced with dummy cannulas.

Immunofluorescence

Mice were anesthetized using pentobarbital sodium (75 mg/kg) and infused with saline, followed by 4% formaldehyde from the base of the left ventricle. Brains were dissected and postfixed for 24 h at 4 ℃ and then dehydrated with a solution of 30% sucrose in 0.1 M PBS at 4 ℃ for at least 3

days. Brains were cut into slices of 40 μm thickness using a freezing microtome (Leica). Slices were washed with phosphate-buffered saline (PBS) and treated with 1% Triton-100, followed by goat serum and incubation with the primary antibody, goat anti-ChAT(1:200; Millipore, AB144P), mouse anti-D28K (1: 1000, Swant, 300) at 4 ℃ overnight. Following incubation, sections were washed three times in PBS. Then, they were incubated with the corresponding fluorescence-conjugated secondary antibody [(Alexa Fluor 488 (1:500; A11034; Invitrogen), Alexa Fluor 594 (1:500; A11005; Invitrogen), (Alexa Fluor 647 (1:500; A32849; Invitrogen)] at room temperature for 2 h. Finally, they were washed three times in PBS and mounted on glass slides with DAPI. Images with fluorescence were captured by fluorescence microscopy (Nikon).

Corticosterone Measurements

To determine the basal hormone plasma levels, mice were housed in an undisturbed environment throughout the night before experiments. Blood sampling was performed in the morning (09:30–10:30). Mouse trunk blood was rapidly collected by decapitation. Blood samples were centrifuged at 1,000 × g for 20 min at 4 ℃. The supernatant was collected, and plasma corticosterone concentrations were measured in duplicate using ELISA kits (Andygene; ADG0121M).

Slice Preparation

The mice were anesthetized with pentobarbital sodium (75 mg/kg), followed by ice-cold oxygenated modified ACSF (containing 220 mM sucrose, 2.5 mM KCl, 1.3 mM $CaCl_2$, 2.5 mM $MgSO_4$, 1 mM NaH_2PO_4, 26 mM $NaHCO_3$, and 10 mM glucose) from the base of the left ventricle and subsequently decapitated, and the brains were quickly dissected and MS/vDB slices (300 mm) were prepared using a VT-1200S vibratome (Leica, Germany) and subsequently transferred to a storage chamber containing normal ACSF (120 mM NaCl, 2.5 mM KCl, 1.2 mM NaH_2PO_4, 2.0 mM $CaCl_2$,

2.0 mM $MgSO_4$, 26 mM $NaHCO_3$, and 10 mM glucose) for a 30-min recovery period at 34 ℃ and subsequently at room temperature (25 ± 1 ℃) for an additional 2–8 h. All solutions were saturated with 95% O_2/5% CO_2 (vol/vol).

Electrophysiological recordings

As described in previous studies, the slices were placed in a recording chamber perfused with ACSF (2 ml/min) at 32–34 ℃. Whole-cell patch-clamp recordings of MS/vDB neurons were obtained under IR-DIC visualization (Zeiss, Axioskop2). Pipettes were pulled using a micropipette puller (P-97, Sutter instrument) with a resistance of 3–6 MΩ. Recordings were obtained using a MultiClamp 700B amplifier and 1440A digitizer (Molecular Device). All analyses were performed using Clampfit 10.2 (Axon Instruments/Molecular Devices) or Minianalysis.

The intrinsic excitability of the neurons was assessed by measuring the firing rate in response to a series of depolarizing pulses in the presence of 20 μM CNQX, 100 μM AP5, and 20 μM BMI. The pipettes were filled with ACSF solution containing 133 mM potassium gluconate, 18 mM NaCl, 0.6 mM EGTA, 10 mM HEPES, 2 mM Mg^{2+}-ATP, and 0.3 mM Na^{+}-GTP (pH: 7.2, 280 mOsm). The steady-state current was injected in +20 pA increments from -60 pA to +220 pA.

sEPSCs were recorded in the presence of the GABAAR antagonist BMI (10 mM). To record sEPSCs, the pipettes were filled with ACSF solution containing 133 mM potassium gluconate, 18 mM NaCl, 0.6 mM EGTA, 10 mM HEPES, 2 mM Mg^{2+}-ATP, and 0.3 mM Na^{+}-GTP (pH: 7.2, 280 mOsm). After the whole cell record was formed, the neurons were held at -70 mV under voltage-clamp mode to record sEPSCs. sIPSCs were recorded at a holding potential of -70 mV with an internal solution containing 140 mM CsCl, 2 mM $MgCl_2$, 1 mM $CaCl_2$, 10 mM EGTA, 10 mM HEPES-CsOH, 2 mM adenosine triphosphate, and 5 mM QX-314. Then, 20 μM CNQX and 100 μM AP5 were added

to the recording solution. sEPSCs and sIPSCs were recorded for 2 min.

To validate modulation of cholinergic neurons with ChR2, eNpHR3.0, iDREADD or eDREADD, whole-cell recordings in gap-free mode were obtained with pipettes filled with a current-clamp internal solution (133 mM potassium gluconate, 18 mM NaCl, 0.6 mM EGTA, 10 mM HEPES, 2 mM Mg^{2+}-ATP, and 0.3 mM Na^{+}-GTP (pH: 7.2, 280 mOsm)). For optogenetics, spikes induced by blue light stimulation in neurons expressing ChR2 were recorded; the frequency of action potential induced by current injection in neurons expressing eNpHR3.0 was compared before, during and after yellow light stimulation. For chemogenetics, in hM3D(Gq) neurons, CNO (5 μM) was bath applied, and changes in action potential were recorded. In hM4D(Gi) neurons, current was injected to induce action potential; then, CNO (5 μM) was bath applied, and changes in action potential were recorded.

Single neuron RNA extraction procedures

To obtain transcriptome data from the different projection single neurons, we applied the recently developed Patch-seq protocol but did not perform electrophysiology recording. [1] We took great care to improve RNA recovery and osmolarity. Glass capillaries (1.2 mm OD, 0.69 mm ID, Sutter Instruments Cat.no. BF120-69-15) were autoclaved before pulling patch-clamp pipettes. All working surfaces that may contact the reagents or solution were RNase-free or cleaned thoroughly with RNase Zap (Life Technologies Cat. AM9780) and DNA-OFF (Takara Cat.no. 9036) before use. Intracellular solution was prepared by dissolving 4 mM KCl, 10 mM HEPES, 0.2 mM EGTA and 111 mM potassium gluconate in RNase-free water in a 200 ml conical flask. The solution was mixed thoroughly, and then 4 mM MgATP, 0.3 mM Na3GTP, 5 mM sodium phosphocreatine (all components from Sigma–Aldrich), and RNase inhibitor were added at a 1:1000 dilution (Takara

Cat. 2313A). The pH was adjusted to 7.40 with RNase-free 0.5 M KOH with the assistance of a dedicated pH meter. Afterward, RNase-free water was added to the solution to achieve the desired volume. The osmolarity of the solution was then carefully checked at approximately 300-310 milliosmoles (mOSM). The solution was stored at -20℃ and was used within a maximum period of 2 weeks.

The cell lysis buffer was prepared using the SMART-Seq HT Kit (Takara Cat. 634437) but without adding 3′ SMART-Seq CDS Primer II A and with a reduction of 5 μl of RNase-free water reserved for the volume of intracellular solution containing the cell samples. The cell lysis buffer was stored in a 200 μl RNase-free tube (Axygen Cat.no. HBDY200UI) on ice. The 3′ SMART-Seq CDS Primer II A was added to the cell lysis buffer before lysis started.

Different from the Patch-seq protocol, the labeled neurons were directly aspirated by the pipettes without recording. The pipette size did not exceed 1 MΩ due to the lack of recording requirements and the large size of cholinergic neurons. During aspiration, if any extracellular contents were observed to enter the pipette, both the pipette and its contents were discarded. The qualified cells were injected into the cell lysis buffer, and each tube contained no more than 5 cells. The samples were dropped into liquid nitrogen and then stored at -80℃. All samples were subsequently converted into cDNA using the SMART-Seq HT Kit within a maximum period of 1 week. Samples with less than approximately 1 ng total cDNA or with an average size less than 1,500 bp were not sequenced. The cDNA library was purified and constructed using the TruePrepTM DNA Library Prep Kit V2 for Illumina (Vazyme Cat.no. TD501-TD503). The range of total length distribution of the DNA library was 300 bp-700 bp. We used the TruePrep Index Kit V2 for Illumina (Vazyme Cat.no. TD202) to perform dual-end index tags. The resulting cDNA libraries were then frozen and

sent for sequencing in 3 separate batches within a maximum period of 2 weeks.

RNA-seq analysis

We performed base calling on the raw image data of the RNA-seq results using Bcl2fastq v2.20.0.422. RNA-seq data were aligned with Mus_musculus_GRCm39.107_Ensembl. For RNA-seq data quality control, FastQC [2] v0.10.1 and Cutadapt [3] v1.9.1 were applied to remove the adapter sequences, low-quality scores (<20) at the 5' or 3' ends or bases containing 'N', and sequences with a trimmed to a length less than 75 bp.

DEGs were analyzed by DESeq2[4] v1.38.3. Genes with $|\log2(\text{fold change})| > 1$ and p value < 0.05 were defined as DEGs in this study.

Supplemental figures and legends

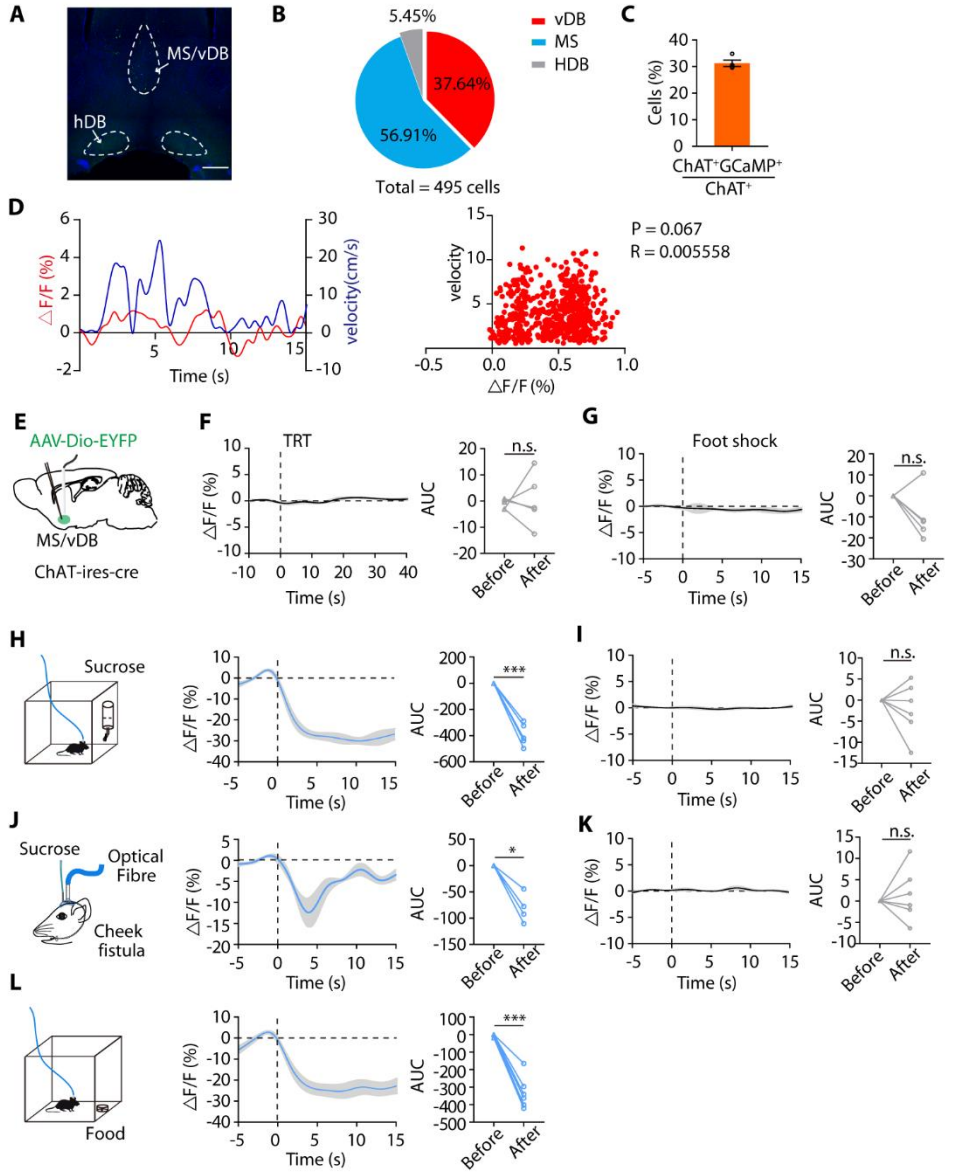

Fig. S1 | Movement does not affect fluorescence intensity recording, and appetitive reward suppresses MS/vDB ChAT neuronal activity. Related to Fig. 1.

(**A**) The expression of GCaMP6m in the MS, vDB and hDB. Scale bar, 200 μm. (**B**) The quantification of GCaMP6m in MS, vDB and hDB, Scale bar, 200 μm. (**C**) The percentage of GCaMP6m-expressing ChAT neurons of total ChAT neurons in the MS/vDB. (**D**) Left, the traces of △F/F (red) aligned to the velocity (blue) of mice; right, the correlation ship of △F/F (red) and velocity (n = 6 mice). (**E**) Schematic for recording of MS/vDB ChAT neurons expression of EYFP.

(**F**) Left, plot of fluorescence intensity aligned to the start of TRT. Right, quantification of the change in fluorescence intensity before and after TRT. n = 5 mice, paired t test. (**G**) Left, plot of fluorescence intensity aligned to the start of footshock. Right, quantification of the change in fluorescence intensity before and after footshock. n = 5 mice, paired t test. (**H**) Left, schematic showing sucrose intake. Middle, plot of Ca^{2+} transients aligned to the start of sucrose intake. Right, quantification of the change in fluorescence intensity before and after sucrose intake. n = 6 mice, paired t test. (**I**) Left, schematic of intraoral sucrose infusion through a cheek fistula. Middle, plot of Ca^{2+} transients aligned to the start of sucrose infusion. Right, quantification of the change in Ca^{2+} transients before and after sucrose infusion. n = 6 mice, paired t test. (**J**) Left, schematic showing food intake. Middle, plot of Ca^{2+} transients aligned to the start of sucrose intake. Right, quantification of the change in calcium signals before and after sucrose intake. n = 6 mice, paired t test. (**K**) Left, plot of fluorescence intensity of MS/vDB ChAT neuron expression of EYFP aligned to the start of sucrose intake. Right, quantification of the change in fluorescence intensity before and after sucrose intake. n = 6 mice, paired t test. (**L**). Left, plot of fluorescence intensity of MS/vDB ChAT neuron expression of EYFP aligned to the start of sucrose delivery. Right, quantification of the change in fluorescence intensity before and after sucrose intake. n = 6 mice, paired t test. *, $p < 0.05$; ***, $p < 0.001$. Data are presented as the mean ± SEM.

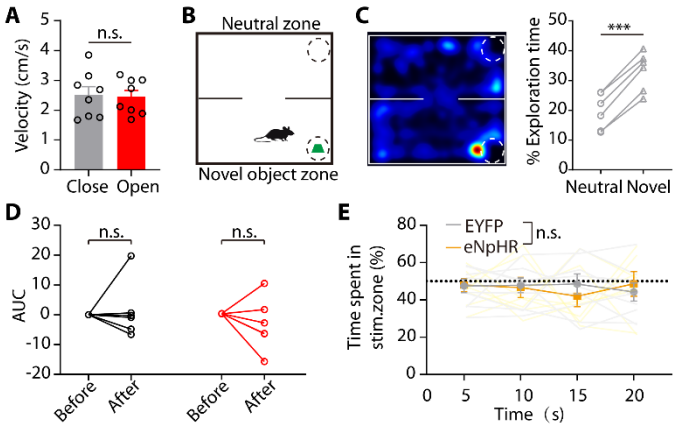

Fig. S2 | MS/vDB ChAT neuronal activity is not involved in novel object recognition and reward. Related to Fig. 3.

(**A**) Mice have similar speed in the closed or open arms in the EPM. n= 8, p = 0.8664, unpaired t test. (**B**) Novel object task design. (**C**) Mice spent significantly more time exploring the novel object than the neutral zone. n= 6, $p < 0.001$, paired t test. (**D**) MS/vDB ChAT neuron activity was not significantly different between the novel object (n= 6, paired t test) and neutral zone (n= 6, paired t test). (**E**) Mice showed no preference for exploration of the light-inhibition side in the RTPP. two-way, repeated-measures ANOVA. ***, $p < 0.001$. Data are presented as the mean ± SEM.

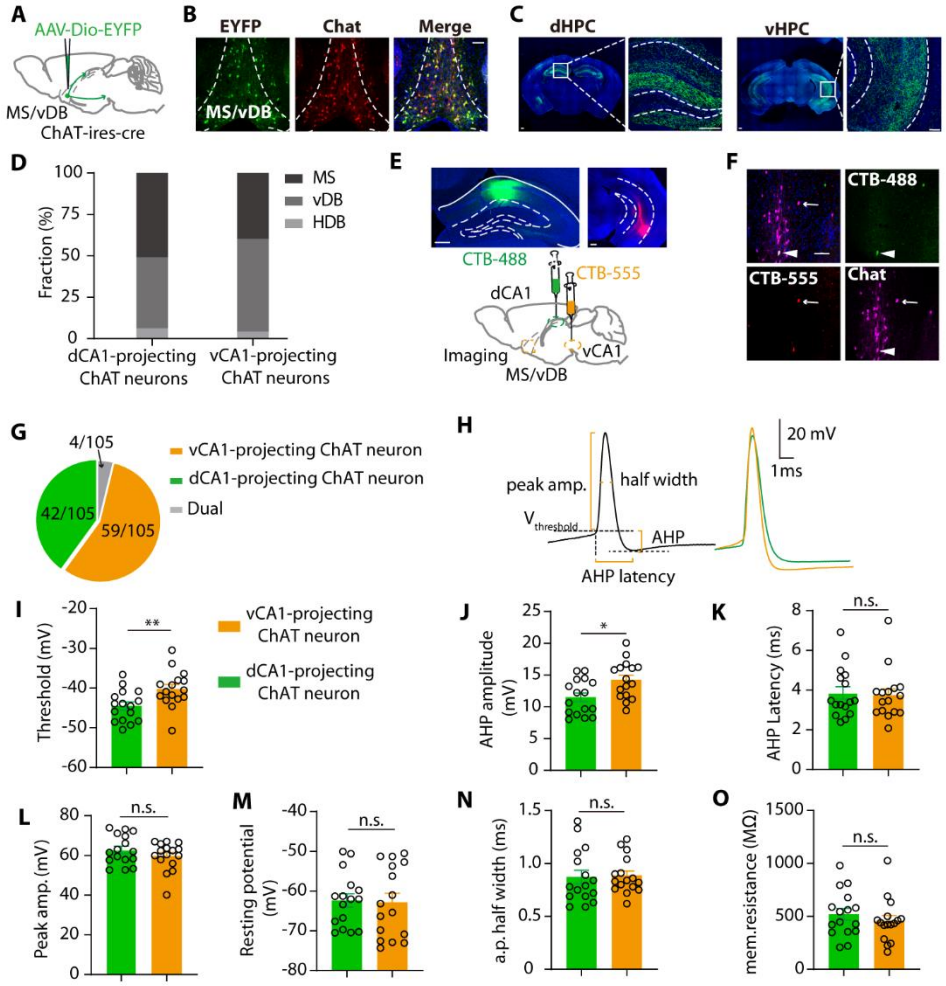

Fig. S3 | dCA1- and vCA1-projecting MS/vDB ChAT neurons are electrophysiologically distinct. Related to Fig. 4.

(**A**) Schematic of the viral vector strategy for tracing MS/vDB ChAT neuronal projections anterogradely. (**B**) Representative image of EYFP expression (green) in MS/vDB ChAT neurons (red). Scale bar, 100 μm. (**C**) Nerve fibers in dHPC (left) and vHPC (right) from MS/vDB ChAT neurons. Scale bar, 200 μm. (**D**) The distribution of dCA1-projecting ChAT neurons and vCA1-projecting ChAT neurons in MS, vDB and hDB. (**E**) Representative images of beads injection sites in the dHPC (CTB-488) and vHPC (CTB-555). Scale bar, 200 μm. (**F**) Retrograde labeling in the MS/vDB. The arrow depicts the colocalization of CTB-488 beads and ChAT neurons (stained by 647 fluorescence), and the triangle depicts the colocalization of CTB-555 and ChAT neurons. Scale

bar, 100 μm. (**G**) Quantitation of MS/vDB ChAT neurons that colocalized with CTB beads injected into the dHPC, vHPC or both. (**H**) Left, schematic defining how certain action potential (a.p.) properties were quantified. All measurements were recorded in the presence of the synaptic blockers NBQX and picrotoxin. AHP: after-hyperpolarization. Right, sample a.p. traces of dCA1- or vCA1-projecting MS/vDB ChAT neurons. (**I**) a.p threshold, unpaired t test. (**J**) AHP amplitude, unpaired t test. (**K**) AHP latency, unpaired t test. (**L**) Peak a.p. amplitude. unpaired t test. (**M**) Resting membrane potential. unpaired t test. (**N**) a.p. half width. unpaired t test. (**O**) Membrane resistance. unpaired t test. dCA1-projecting MS/vDB ChAT neurons n = 16, vCA1-projecting MS/vDB ChAT neurons n=16. *, $p < 0.05$; **, $p < 0.01$. Data are presented as the mean ± SEM.

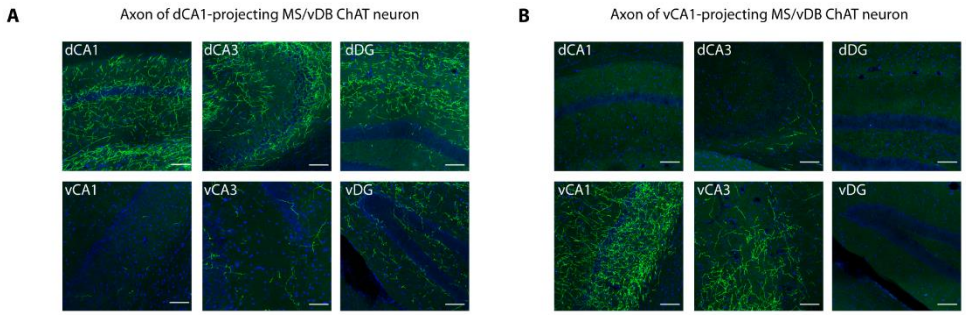

Fig. S4 | dCA1- and vCA1-projecting MS/vDB ChAT neurons exhibit different inputs to the subregions of dHPC and vHPC. Related to Fig. 4.

(**A**) The distribution of dCA1-projecting MS/vDB ChAT axons in dCA1, dCA3, dDG, vCA1, vCA3 and vDG, Scale bar, 200 μm. (**B**) The distribution of vCA1-projecting MS/vDB ChAT axons in dCA1, dCA3, dDG, vCA1, vCA3 and vDG, Scale bar, 200 μm.

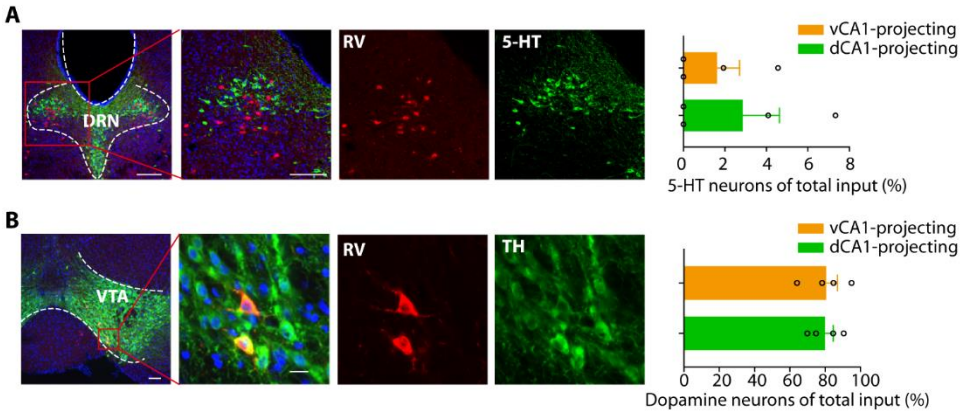

Fig. S5 | dCA1- and vCA1-projecting MS/vDB ChAT neurons exhibit similar inputs from the DRN and VTA. Related to Fig. 4.

(**A**) Left, images of DRN neurons sending input to MS/vDB ChAT neurons. Red represents rabies+ input cells, and green represents serotonin neurons. Scale bar, 100 μm. Right, the ratio of serotonin neurons among the DRN input cells of dCA1- and vCA1-projecting MS/vDB ChAT neurons. (**B**) Left, images of VTA neurons sending input to MS/vDB ChAT neurons. Red represents rabies^{+} input cells, and green represents dopamine neurons. Scale bar, 100 μm. Right, the ratio of dopamine neurons among the VTA input cells of dCA1- and vCA1-projecting MS/vDB ChAT neurons. Data are presented as the mean ± SEM.

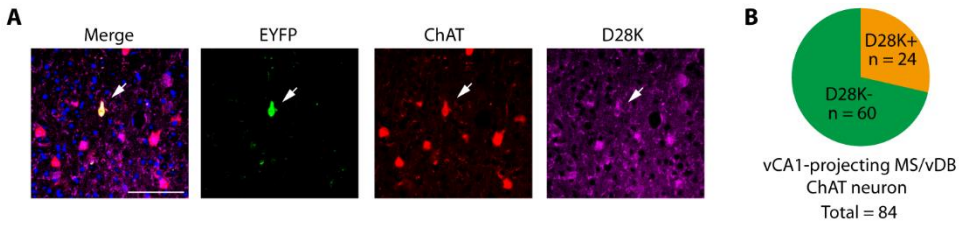

Fig. S6 | The expression of D28K in vCA1-projecting MS/vDB ChAT neurons.

(**A**) Left, images of vCA1-projecting MS/vDB ChAT neurons that express D28K. Green represents vCA1 input cells, red represents ChAT neurons and purple represents D28K. Scale bar, 100 μm. (**B**) The ratio of vCA1-projecting MS/vDB ChAT neurons that express D28K, n = 84 from 3 mice.

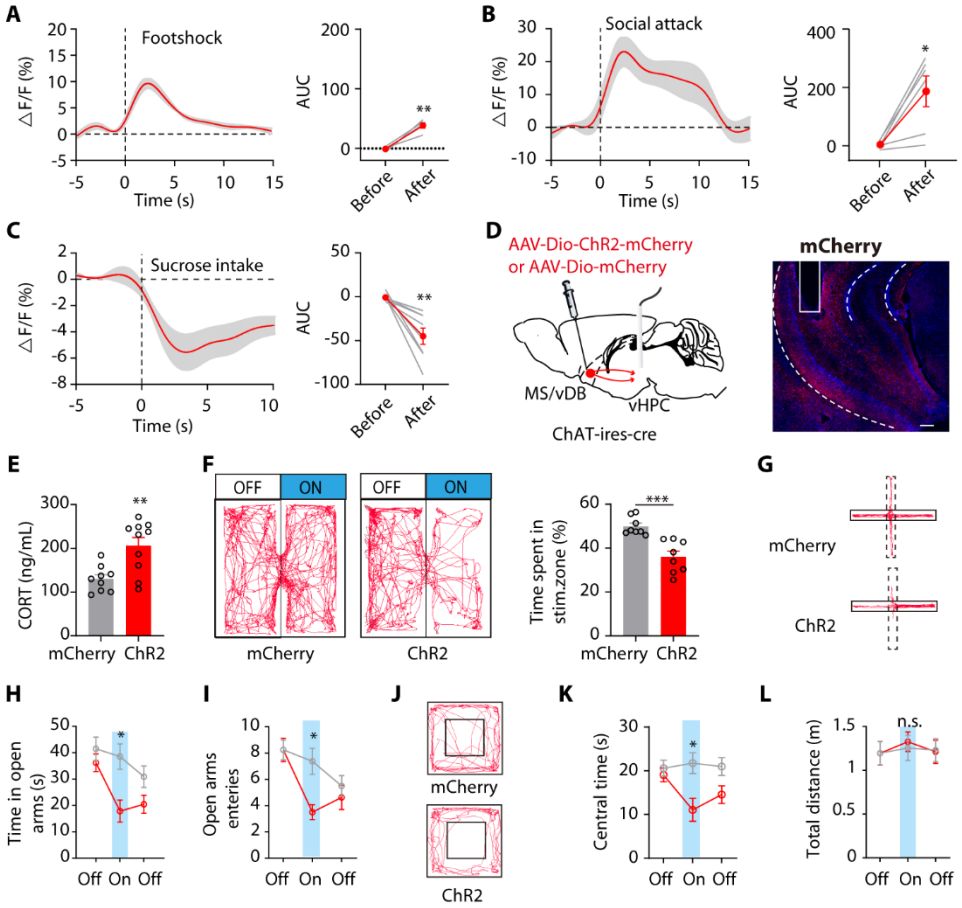

Fig. S7 | The ChAT$^{MS\text{-}vHPC}$ cholinergic projection transmits a negative valence signal. Related to Fig. 5

(**A**) Plot (left) of Ca^{2+} transients aligned to the start of footshock and quantification of change (right) in Ca^{2+} signals before and after footshock. n= 5, paired t test. (**B**) Plot of Ca^{2+} transients aligned to the start of social attack and quantification of the change in Ca^{2+} signals before and after social attack. n= 6, paired t test. (**C**) Plot of Ca^{2+} transients aligned to the start of sucrose intake and quantification of the change in Ca^{2+} signals before and after sucrose infusion. n= 8, paired t test. (**D**) Left, schematic for unilateral optogenetic activation of MS/vDB-vHPC cholinergic projections. Right, representative placement of fiber optic. Scale bar, 20 μm. (**E**) Optogenetic stimulation of MS/vDB-vHPC cholinergic projections increased CORT. mCherry n = 9, ChR2 n = 10, unpaired t

test. (**F**) Left, representative locomotor traces of mCherry- and ChR2-mice in RTPA. Right, light activation of MS/vDB-vHPC cholinergic projections results in place aversion in ChR2- mice. mCherry n = 8, ChR2 n = 8, unpaired t test. (**G**) Representative animal tracks during the illumination epoch within EPM for ChR2-mouse and mCherry-mouse. (**H**) During the illumination epoch (On), ChR2-mice spent significantly less time in the open arms relative to mCherry-mice. two-way ANOVA with Bonferroni post hoc tests. (**I**) During the illumination epoch (On), ChR2 mice show a lower probability of open-arm entry relative to mCherry mice. two-way ANOVA with Bonferroni post hoc tests. (**J**) Representative animal tracks during the illumination epoch in the open-field chamber for a ChR2-mouse and an mCherry-mouse. (**K**) During the illumination epoch (On), ChR2-mice spent significantly less time exploring the center of the open field relative to mCherry-mice. two-way ANOVA with Bonferroni post hoc tests. (**L**) Photostimulation did not alter the distance traveled for either group. two-way ANOVA with Bonferroni post hoc tests. *, $p < 0.05$; **, $p < 0.01$; and ***, $p < 0.001$. Data are presented as the mean ± SEM.

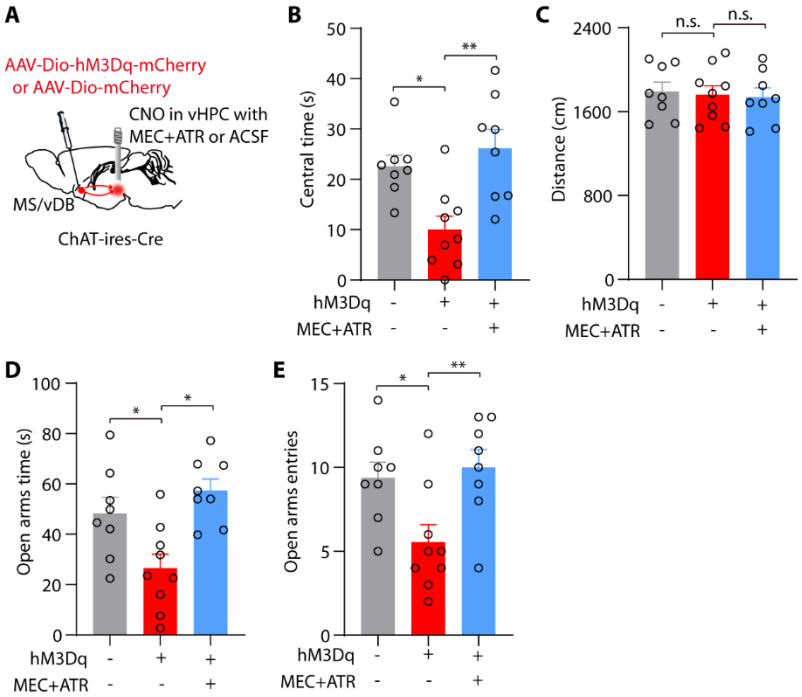

Fig. S8 | Chemogenetic activation of MS/vDB-vHPC cholinergic projections heighten anxiety

levels in mice by increasing ACh release. Related to Fig. 5

(**A**) Schematic for inhibition of ACh receptors in the vHPC prior to chemogenetic activation of MS/vDB-vHPC cholinergic projections. (**B**) Application of cholinergic receptor antagonists ATR+MEC into the vHPC blocked the chemogenetic activation-induced reduction of center exploration in the OFT. mCherry + ACSF n = 8, hM3Dq + ACSF n = 9, hM3Dq + (ATR+MEC) n = 8. (**C**) Application of cholinergic receptor antagonists had no effect on locomotion. (**D**) Application of cholinergic receptor antagonists into the vHPC blocked the chemogenetic activation-induced reduction of open arms exploration in the EPM. (**E**) Application of cholinergic receptor antagonists into the vHPC blocked the chemogenetic activation-induced reduction of open arms entries in the EPM. One-way ANOVA with Tukey's multiple-comparison test. *, $p < 0.05$; **, $p < 0.01$. Data are presented as the mean ± SEM.

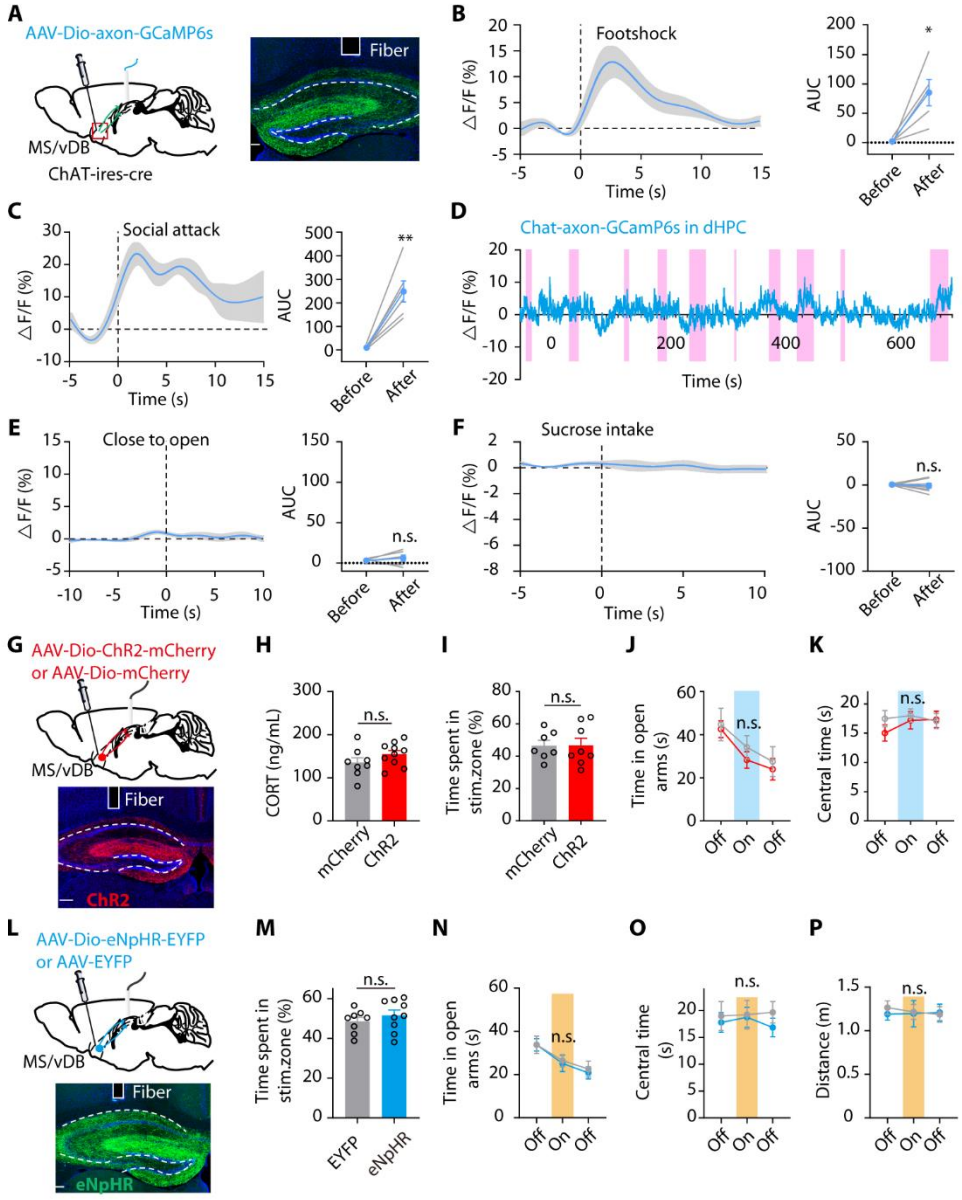

Fig. S9 | Modulation of MS/vDB cholinergic input to the dHPC had no effect on anxiety-like behaviors. Related to Fig. 5.

(**A**) (left) Schematic for recording the activity of the MS/vDB-dHPC cholinergic projection. (right) Representative placement of fiber optic in dHPC. Scale bar, 200 μm. (**B**) Plot of Ca^{2+} transients aligned to the start of footshock and quantification of change in Ca^{2+} signals before and after footshock. n= 5, paired t test. (**C**) Plot of Ca^{2+} transients aligned to the start of social attack and quantification of the change in Ca^{2+} signals before and after social attack. n= 6, paired t test. (**D**) Example of MS/vDB-dHPC cholinergic fiber activity within the EPM. Pink columns reflect the time

the mouse entered the open arms. (**E**) Plot of Ca^{2+} transients aligned to the start of open arm entry and quantification of change in calcium signals before and after open arm entry. n= 6, paired t test. (**F**) Plot of Ca^{2+} transients aligned to the start of sucrose intake and quantification of the change in Ca^{2+} signals before and after sucrose infusion. n= 7, paired t test. (**G**) Schematic for unilaterally optogenetic activation of MS/vDB-dHPC cholinergic projections (top). Representative placement of fiber optic (down). Scale bar, 200 μm. (**H**) Optogenetic stimulation of MS/vDB-dHPC cholinergic projections had no effect on mouse CORT. mCherry n= 8 ChR2 n = 10, unpaired t test. (**I**) Optogenetic stimulation of MS/vDB-dHPC cholinergic projections did not induce place aversion. mCherry n= 7 ChR2 n = 8, unpaired t test. (**J, K**) Lumination of MS/vDB-dHPC cholinergic projections showed little effect on open arm time (**J**) and open arm entries (**K**). (**L**) Schematic for bilateral optogenetic silencing of MS/vDB-dHPC cholinergic projections (top). Representative placement of fiber optic (down). Scale bar, 200 μm. (**M**) Optogenetic inhibition of MS/vDB-dHPC cholinergic projections did not induce place aversion. EYFP n= 8 ChR2 n = 9, unpaired t test. (**N, O**) Inhibition of MS/vDB-dHPC cholinergic projections showed little effect on time spent in open arms (**N**) in EPM and central time in OFT (**O**), (**P**) Inhibition of MS/vDB-dHPC cholinergic projections showed little effect on locomotion. $p > 0.999$. *, $p < 0.05$; **, $p < 0.01$. Data are presented as the mean ± SEM.

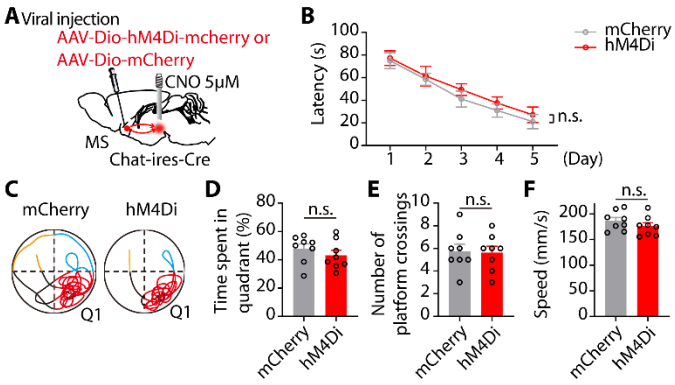

Fig. S10 | Modulation of MS/vDB cholinergic input to the vHPC had no effect on spatial learning. Related to Fig. 5.

(**A**) Schematic for injection of control and hM4Di virus in MS/vDB and CNO delivery in vHPC for chemogenetic inhibition of the MS/vDB-vHPC cholinergic pathway. (**B**) Chemogenetic inhibition of the MS/vDB-vHPC cholinergic pathway did not change the escape latency during acquisition training. mCherry n= 8, hM4Di n = 8, two-way repeated-measures ANOVA. (**C**) Representative traces of swimming paths in the probe trial. (**D**) Chemogenetic inhibition of the MS/vDB-vHPC cholinergic pathway during training had no effect on the time spent in Q1. (**E**) Chemogenetic inhibition of the MS/vDB-vHPC cholinergic pathway during training had no effect on the number of platform crossings. (**F**) Chemogenetic inhibition of the MS/vDB-vHPC cholinergic pathway had no effect on the speed in the MWM. Data are presented as the mean ± SEM.

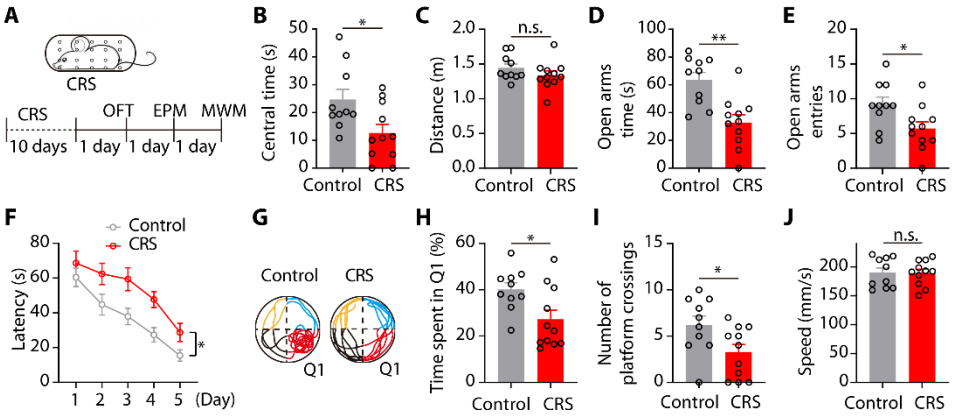

Fig. S11 | Chronic stress induces anxiety-like behaviors and impairs mouse spatial learning and memory. Related to Fig. 6.

(**A**) The timeline of experiments. (**B-C**) Chronic stress mice spent less time in the center (**B**) but had similar locomotion (**C**), during the OFT. (**D, E**) Chronic stress mice spent less time in the open arms

(**D**) and had fewer open arm entries (**E**). (**F**) Chronic stress mice needed more time to escape during the training session, two-way ANOVA. (**G**) Representative traces of swimming paths in the probe trial. (**H**) Chronic stress mice spent less time in Q1. (**I**) Chronic stress mice showed a smaller number of platform crossings. (**J**) Chronic stress mice had swimming speeds similar to those of control mice. *, $p < 0.05$; **, $p < 0.01$. Data are presented as the mean ± SEM.

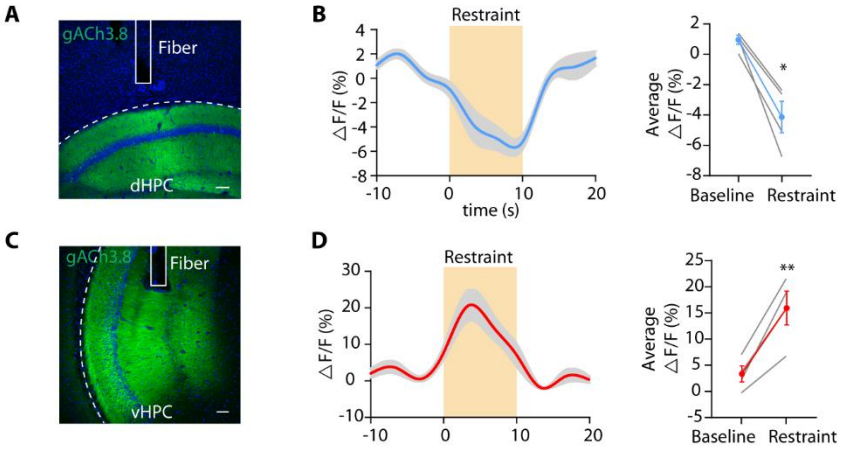

Fig. S12 | The release of ACh in dHPC and vHPC in response to acute restraint stress. Related to Fig. 6.

(**A**) A representative image validates gACh3.8 expression (green) and optical fiber tract above the dHPC. Scale bar, 100 μm. (**B**) Left, plot of fluorescence transients across animals aligned to the start of restraint stress. Right, the change in fluorescence transients before and during restraint stress. n = 4 mice, $p = 0.0131$, paired t test. (**C**) A representative image validates gACh3.8 expression (green) and optical fiber tract above the vHPC. Scale bar, 100 μm. (**D**) Left, plot of fluorescence transients across animals aligned to the start of restraint stress. Right, the change in fluorescence transients before and during restraint stress. n = 4 mice, paired t test. *, $p < 0.05$; **, $p < 0.01$. Data are presented as the mean ± SEM.

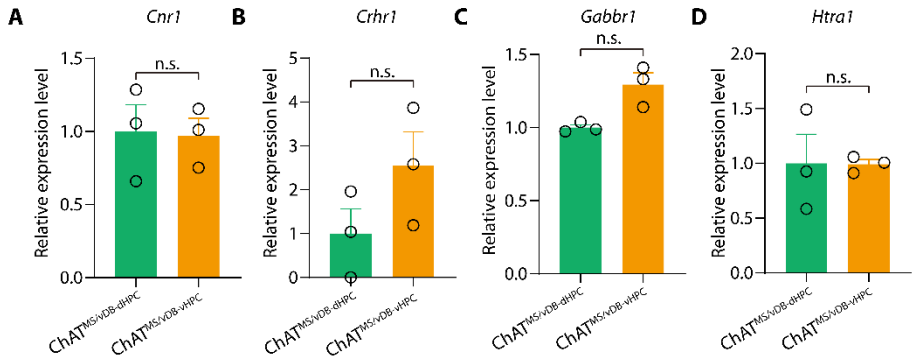

Fig. S13 | The relative mRNA expression of *Cnr1*(Cannabinoid Receptor 1, A), *Crhr1*(corticotropin-releasing hormone receptor type 1, B), *Gabbr1*(Gamma-Aminobutyric Acid B Receptor 1, C) and *Htra1* (serotonin 1A receptor, D) in ChAT$^{MS\text{-}dHPC}$ and ChAT$^{MS\text{-}vHPC}$ neurons. unpaired t test. Data are presented as the mean ± SEM.

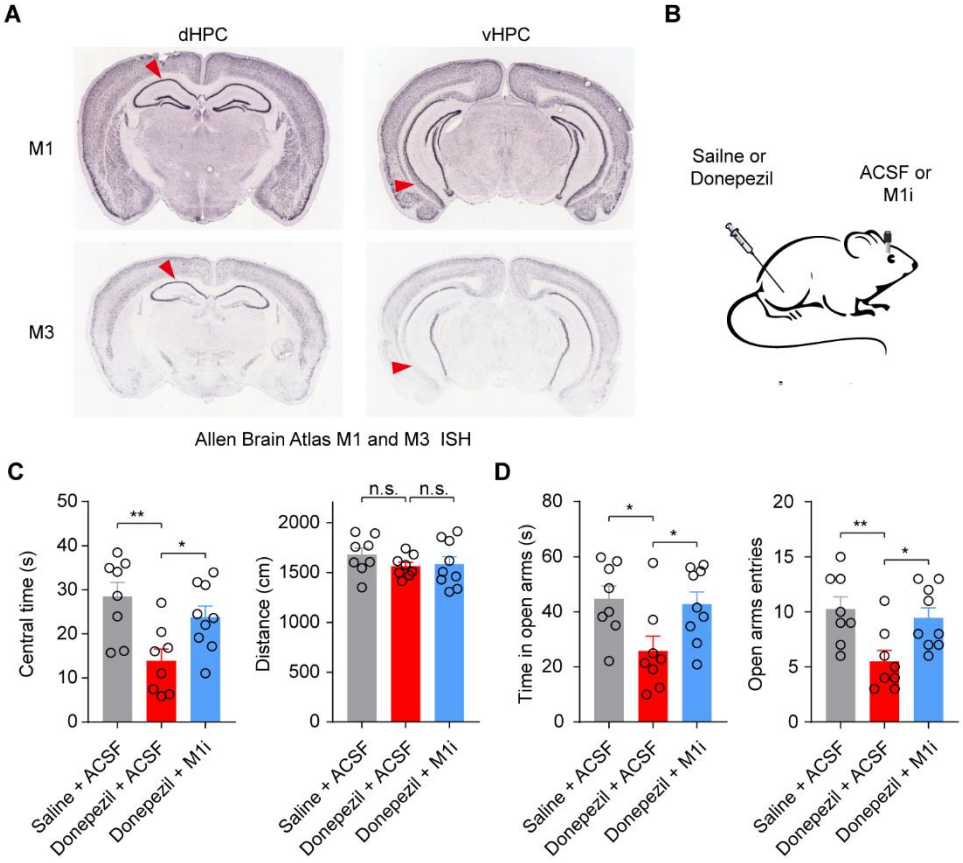

Fig. S14 | Donepezil promotes anxiety-like behavior through M1 receptors in the vHPC region.

Related to Fig. 8.

(**A**) M1 and M3 receptor expression in the hippocampus from **Allen Brain Atlas ISH data**. (**B**) Scheme of the drug delivery strategy. (**C**) Left, intraperitoneal administration of donepezil in mice reduces center time in OFT, which is blocked by intra-vHPC M1i treatment (Saline + ACSF n = 8, Donepezil + ACSF n = 8, Donepezil + M1i n = 9). Right, drug delivery had no effect on mouse locomotion. (**D**) Intraperitoneal administration of donepezil in mice reduced the time spent and entry into the open arms of the EPM, which was blocked by intra-vHPC M1i treatment. One-way ANOVA with Tukey's multiple-comparison test. *, $p < 0.05$; **, $p < 0.01$, ***, $p < 0.001$. Data are presented as the mean ± SEM.

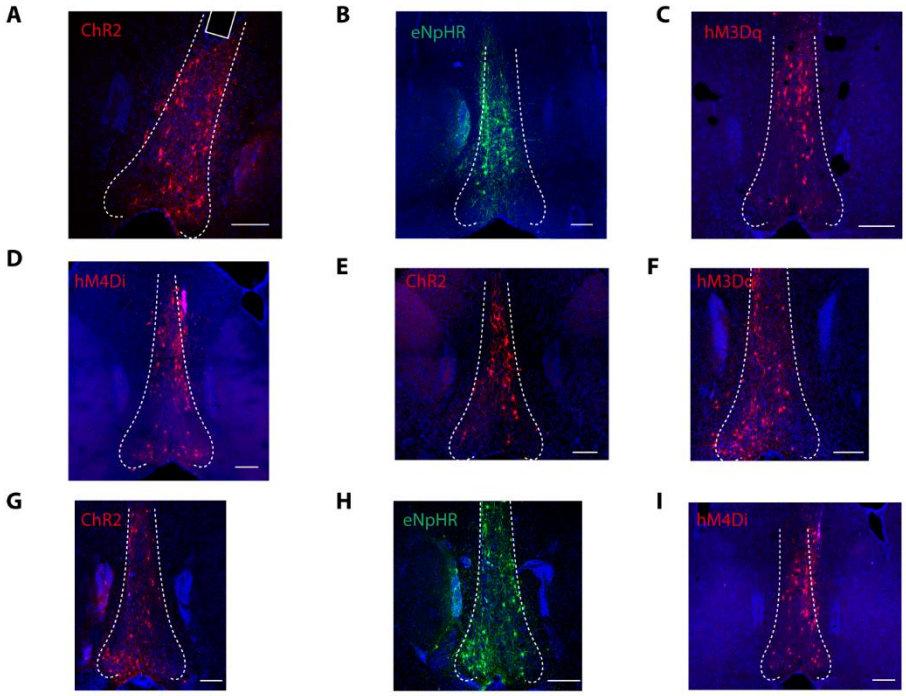

Fig. S15 | Virus expression in the MS/vDB region.

(**A**) The expression of ChR2 in the MS/vDB region, related to Fig. 3H. Scale bar, 200 μm. (**B**) The expression of eNpHR in the MS/vDB region, related to Fig. 5F. Scale bar, 200 μm. (**C**) The expression of hM3Dq in the MS/vDB region, related to Fig. 7A. Scale bar, 200 μm. (**D**) The

expression of hM4Di in the MS/vDB region, related to Fig. 7G. Scale bar, 200 μm. (**E**) The expression of ChR2 in the MS/vDB region, related to Fig. S7D. Scale bar, 200 μm. (**F**) The expression of hM3Dq in the MS/vDB region, related to Fig. S8A. Scale bar, 200 μm. (**G**) The expression of ChR2 in the MS/vDB region, related to Fig. S9G. Scale bar, 200 μm. (**H**) The expression of eNpHR in the MS/vDB region, related to Fig. S9L. Scale bar, 200 μm. (**I**) The expression of hM4Di in the MS/vDB region, related to Fig. S10A. Scale bar, 200 μm.